Developing Analytical Model for Nighttime Cooling of Internal Thermal Mass

Wentao Wu[1,2], Jingru Benner[3], Zhiwen Luo[4,5]*

[1]*Department of Civil and Natural Resources Engineering, University of Canterbury, Christchurch, 8041, New Zealand*
[2]*Department of Civil & Architectural Engineering, College of Engineering, Tennessee State University, Nashville, TN 37209, USA*
[3]*College of engineering, Western New England University, Springfield, MA 01119, USA*
[4]*Welsh School of Architecture, Cardiff University, Cardiff, United Kingdom*
[5]*School of the Built Environment, University of Reading, Reading, United Kingdom*

[*]***Corresponding author**: Wentao Wu, wentao.wu@canterbury.ac.nz*

Abstract

Nighttime mechanical ventilation of internal building thermal mass has the potential to create energy flexibility by shifting peak cooling demand. The research on nighttime cooling of internal thermal mass is limited due to lacking simplified models by considering mass dimension and real-world discrete climate data like outdoor air temperatures. This study develops an analytical model for nighttime cooling of internal thermal mass with a constant air change rate and hourly varied air temperatures. The analytical model is verified by both numerical, conduction transfer function methods, and ANSI/ASHRAE Standard 140-Case 600. The analytical model is applied to quantify the free cooling energy storage in 48 selected U.S. cities in different climate zones and in the 16 climate zones of California. Among the 48 cities, the maximum free cooling energy storage is reported in Santa Fe, NM with a total free cooling energy storage of 19.1 kWh m^{-2} a^{-1} and a net free cooling energy storage of 3.88 kWh m^{-2} a^{-1}. Coastal regions in California are not suitable for nighttime ventilation of internal thermal mass. The maximum total free cooling energy storage in California achieves 27.5 kWh m^{-2} a^{-1}, while the maximum net free cooling energy storage is 6.11 kWh m^{-2} a^{-1}. The analytical model has a potential to be integrated into whole building energy simulation software to improve the calculation of the effect of internal thermal mass.

Key words: energy flexibility; sensible heat storage; CFD; thermal inertia; night cooling; night ventilation.

1. Introduction

The U.S. has committed to joining the global efforts to reach net-zero emissions by 2050 in the 26th Conference of the Parties (COP26). A key pathway toward carbon neutrality is to increase the use of renewable energy sources. The intermittency and fluctuation of onsite renewable energy sources may lead to imbalance between supply and demand. Demand-side energy flexibility with intermediate energy storage is considered a promising solution to alleviate the supply and demand mismatch [1]. Buildings can play an important role to create demand-side energy flexibility by transforming massive structures into thermal mass to store thermal energy [2]. Thermal mass has the capacity to absorb sensible heat during the daytime and release it during the nighttime. The time lag of heat absorption and release shifts the peak thermal load in time and creates energy flexibility [3]. The amount of energy flexibility created by thermal mass alone might be relatively small due to its varied ability to shift heating and cooling demand in different climates [4].

The capacity of thermal mass to shift cooling demand depends on climates. In cold climates,

thermal mass on walls might increase building cooling demand in summer [5]. In warm and mild climates, thermal mass on walls is reported to have low influence on energy demand reduction [6]. In hot climates, high thermal mass of insulated concrete wall increases cooling energy demand as high ambient temperature causes more heat stored during daytime than that released during nighttime [7]. An effective measure to increase the heat release from thermal mass is nighttime cooling [8]. Cool outdoor air can be directly induced to flush the thermal mass and create a heat sink to absorb space heat gains via convection and radiation in the following daytime. Nighttime cooling of thermal mass has the potential to reduce the need for compressor-based cooling energy demand [9]. The efficiency of nighttime cooling is most effective when night-time temperatures are below 20°C, summer diurnal temperature swings are between 15-20°C, and maximum daytime temperature is between 30 and 36°C [10]. A review [11] of related research undertaken between 1997 and 2017 reveals that most work has been done to investigate the energy demand reduction of nighttime cooling of external thermal mass on walls. The external thermal mass is exposed to varied outdoor climate conditions and the heat sink generated in the nighttime might be filled too rapidly in the morning to shift the peak cooling load in the afternoon. One way to expand the lifetime of the heat sink is to use internal thermal mass on the floor. The presence of internal thermal mass can increase the building time constant by up to 42%, which is calculated as the time needed to reach 63.2% of the temperature change between two steady states and measures the ability of thermal mass to time-shift cooling load [12]. A question remains unanswered is: what is the capacity of nighttime cooling of internal mass to reduce energy demand in different U.S. climates?

Limited research on nighttime cooling of internal thermal mass is attributed to the lack of simplified but accurate models to quantify the cooling demand reduction under realistic climate conditions [13,14]. In-situ measurements provide the most realistic quantification of the cooling demand reduction of internal thermal mass. Experiments carried out in two real-scale buildings showed that the use of thermal mass reduced the cooling energy demand by 67% to 75% during 14 days with only slight diurnal temperature variations [15]. However, measuring cooling energy storage is challenging due to difficulties in placing sensors in thermal mass. In most experiments, only air temperatures are measured and it is difficult to separate the influence of thermal mass from other impact factors [16]. Whole building energy simulation software like EnergyPlus [17] and REGCAP [18] are suitable to investigate the transient behavior of internal thermal mass and nighttime ventilation. However, in EnergyPlus, internal thermal mass is either simplified as interior construction materials with an effective area or lumped into the zone air with a capacitance multiplier. The oversimplification might lead to overestimation of energy storage of internal thermal mass that behaves superficially energy efficient. In REGCAP, the internal thermal mass is described with an empirical relationship that scales with floor area. The empirical relationship is based on the concept of the building time constant and does not consider the effect of thermal properties. In most whole building energy simulation software, the thermal mass dimension is completely ignored [19]. Reduced-order models are developed to consider details of internal thermal mass and nighttime cooling. Thermal quadrupole approach [20] can be implemented to calculate thermal energy storage in internal thermal mass. The approach is based on the analytical solution of one-dimensional heat transfer in an infinitely large solid plane, and the boundary conditions are limited to sinusoidal signals. Numerical methods such as finite element [21] or finite difference [22] can be used to quantify the energy demand reduction with internal thermal mass under realistic temperature boundary conditions. The drawback of numerical methods is the requirement of a small time-step to ensure numerical stability, which increases the computational

time [23]. A case study of monthly temperature variation can take up to days to complete the computation. Another approach that is essentially similar to numerical methods is the RC thermal model [24]. A reduced-order RC (2R2C) model was adopted to study the performance of internal thermal mass and results showed that 'building as battery' efficiency is between 40% and 80% depending on the insulation level [25]. A limitation of the 2R2C model is the short prediction time span of up to 12 h. An alternative reduced-order model is to directly derive analytical solutions to the time-dependent heat conduction equation in the internal thermal mass [26]. The state-of-the-art analytical models are limited to simplified boundary conditions. A typical example is to use a sinusoidal function to approximate real-world diurnal outdoor air temperature variations [27]. The sinusoidal approximation cannot reflect the actual complexity of time-varying temperature boundary conditions [4], for example, the nighttime air temperatures are hourly-varied values and the daytime air temperature is the constant setpoint value. To deal with the difference in the nighttime and daytime temperature boundary conditions, Yang and Li [28] developed nighttime and daytime analytical models separately by expressing the outdoor temperature as a sinusoidal profile with a frequency of 24 h. The analytical model is developed for zero-dimensional thermal mass during a period of 24 h. It is in urgent need to develop a simplified mathematical model for nighttime cooling of internal thermal mass to consider mass details and real weather data. The question is how to develop the model by considering mass dimension and real-world weather data, for example, discrete (hourly varied) air temperatures?

In summary, much research has been done to investigate the nighttime cooling of external thermal mass on walls. The research gap is to understand the potential of nighttime cooling of internal thermal mass to reduce cooling demand in different climates. An urgent need is to develop a simplified mathematical model for nighttime cooling of internal thermal mass by considering mass dimension and real-world weather data, e.g., discrete air temperatures in a span of a year. The detailed objectives of this study include: 1) developing a one-dimensional analytical model for nighttime cooling of internal thermal mass with annually discrete air temperature boundary conditions; the model will be validated against numerical simulations, traditional conduction transfer function (CTF) method [29], and ANSI/ASHRAE Standard 140 -2017 [30]; 2) quantifying cooling demand reduction with nighttime cooling of internal thermal mass in different climates. This study will provide a new method to assess the efficiency of nighttime ventilation of internal thermal mass to create energy flexibility [31] and enhancing the utilization of renewable energy [32] . The validated analytical solution could also be used for model predictive control of thermal mass [33] and potentially be integrated into whole building energy simulation software.

2. Materials and methods

The nighttime cooling in this study refers to a system that supplies unconditioned outdoor air into the space to directly cool the concrete floor slab that is the internal thermal mass (Fig. 1a). During the nighttime period, the supply air temperature is hourly varied. In the following daytime period, the slab acts as a heat sink to absorb part of the space heat gains via convection and radiation (Fig. 1b); the air temperature distribution in the space is uniform and equal to a constant setpoint temperature [28]. The daytime air conditioning and nighttime ventilation are provided by a constant air volume system. The heat transfer in the slab is one-dimensional along the vertical direction [34] and the bottom of the slab is well insulated. The slab is a single-layer material. The heat transfer between the slab and the air through radiation and convection is described by a total heat transfer coefficient.

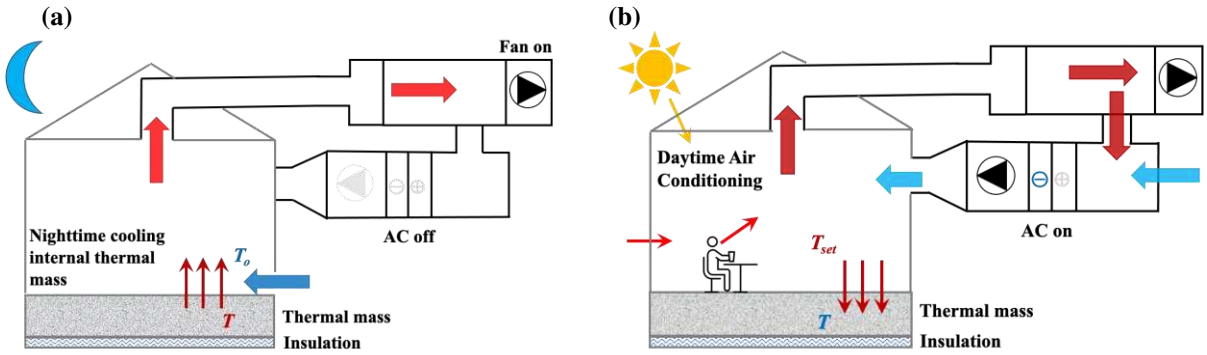

Fig. 1. (a) Nighttime cooling of internal thermal mass and (b) daytime air conditioning. *T* is the thermal mass temperature field; T_o is the nighttime hourly-varied supply air temperature; T_{set} is the daytime setpoint temperature of the conditioned space.

The heat balance for a building with nighttime cooling of internal thermal mass can be described by the following equations presented by Yang and Li [28]:

$$Q_{cl} + Q_{wr} + Q_{win,cond} + Q_{win,sol} + Q_i + Q_{inf} + Q_{itm} = 0 \quad (1)$$

$$\rho_a c_a q_v (T_o - T_{room}) + Q_{itm} + Q_{wr} + Q_{win,cond} + Q_i + Q_{inf} = 0 \quad (2)$$

Equation (1) describes the heat balance during the daytime, where Q_{cl} is the cooling demand (W), Q_{wr} is the conduction cooling load through walls and roof (W), $Q_{win,cond}$ is the conduction cooling load through windows (W), $Q_{win,sol}$ is the cooling load due to solar heat gain through windows (W), Q_i is the cooling load due to internal heat gains (W), Q_{inf} is the infiltration heat gain (W), and Q_{itm} is the cooling load due to heat absorption or release from the internal thermal mass (W). The room air and the internal thermal mass exchange heat through convection and radiation. The total heat absorption or release from thermal mass is calculated as $h_i A_i (T_{surf} - T_{room})$, *where* h_i is the total heat transfer coefficient above the internal thermal mass (W m^{-2} K^{-1}), A_i is the total area of the internal thermal mass (m^2), T_{surf} is the surface temperature of the internal thermal mass (K), and T_{room} is the air temperature in the room (K). Equation (2) describes the heat balance during the nighttime and the first term is the supplied nighttime cooling, where ρ_a and c_a is the density (kg m^{-3}) and specific heat (J kg^{-1} K^{-1}) of air, respectively. The nighttime ventilation rate is q_v (m^3 s^{-1}).

The temperature field in the internal thermal mass is described by the following equation with Robin boundary conditions:

$$\rho c \frac{\partial T}{\partial t} = \frac{\partial^2 T}{\partial y^2} \quad (3)$$

$$-\lambda \frac{\partial T}{\partial y}\Big|_{y=L} = h_i [T(y = L, t) - T_r(t)] \quad (4)$$

$$\lambda \frac{\partial T}{\partial y}\Big|_{y=0} = 0 \quad (5)$$

Equation (3) assumes one-dimensional heat conduction in the internal thermal mass, where *T* is the slab temperature field (K), *y* is the vertical distance from the bottom of the internal thermal mass (m), *t* is time (s), ρ and *c* is the density (kg m^{-3}) and specific heat (J kg^{-1} K^{-1}) of the internal thermal mass, respectively. Equation (4) describes the heat exchange between the internal thermal

mass and the supply air temperature T_r (K), where, λ is the thermal conductivity (W m^{-1} K^{-1}) of the internal thermal mass, and L is the total slab thickness (m). T_r is a combination of unconditioned nighttime outdoor air temperatures and the daytime setpoint temperature of the conditioned space. T_r equals to the hourly varied temperature (T_o) of the outdoor air that is supplied to directly cool the slab in the nighttime period and is the setpoint temperature of the space in the daytime period (T_{set}) (Fig. 2). T_r can be described using the step function:

$$T_r(t) = [H(t) - H(t-t_1)]\,T_{r,1} + [H(t-t_1) - H(t-t_2)]\,T_{r,2} + \cdots + [H(t-t_{M-2}) - H(t-t_{M-1})]\,T_{r,M-1} + H(t-t_{M-1})T_{r,M} \quad (6)$$

$$H(t) = \begin{cases} 0 & t \le 0 \\ 1 & t > 0 \end{cases} \quad (7)$$

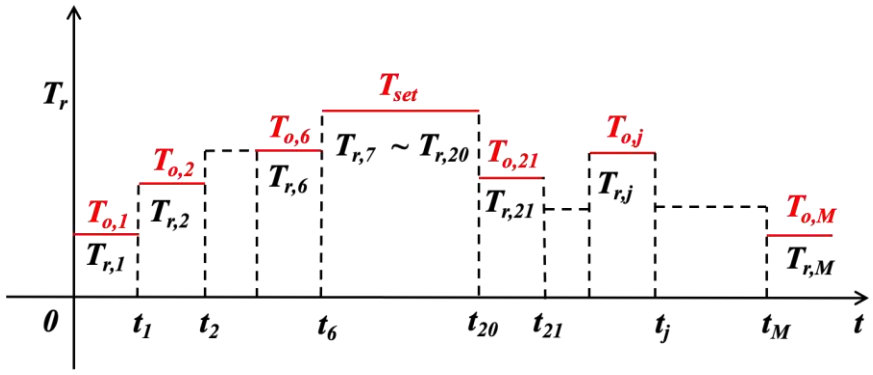

Fig. 2. Hourly varied air temperature.

Equation (5) describes a perfect insulation of the bottom of the internal thermal mass. The initial temperature of the internal thermal mass is set equal to the initial air temperature (T_{set}) and the effect of the initial temperature can be eliminated by periodic calculations.

2.1 Analytical model for nighttime cooling of internal thermal mass

The challenge to derive the analytical solution of equation (3) is the inhomogeneous and time-dependent boundary condition (6) that has discrete free-stream temperatures T_r. When separation of variables is applied, the first derivative of T_r will be introduced into the equation system. Since T_r is discrete and varies hourly in this study, its first derivative requires the use of Dirac delta function:

$$\frac{dT_r}{dt} = \delta(t)T_{r,1} + \sum_{m=1}^{M-1} \delta(t-t_m)\left[T_{r,m+1} - T_{r,m}\right] \quad (8)$$

$$\delta(t) = \begin{cases} 0 & t \neq 0 \\ 1 & t = 0 \end{cases} \quad (9)$$

where, M is the total number of days for nighttime cooling. The analytical solution can be sought by applying shifting function method [35], separation of variables, Fourier series expansion and variation of parameters (VOP) method [26] to the equations (4-9) normalized with:

$$\theta = \frac{T-T_{set}}{T_{set}}, \quad \tau = \frac{\alpha t}{L^2}, \quad \eta = \frac{y}{L}, \quad Bi = \frac{h_i L}{\lambda}, \quad \theta_r = \frac{T_r - T_{set}}{T_{set}} \quad (10)$$

where α is the thermal diffusivity (m s^{-2}) and equals to $\lambda/\rho c$, Bi is the Biot number that measures the ratio of the thermal resistance in the internal thermal mass to the convection of nighttime cooling at the surface of the internal thermal mass. The detailed derivation is given in Appendix A. The final analytical model is established for nighttime mechanical ventilation of building thermal mass with discrete (hourly varied) temperature boundary conditions:

$$\theta = \sum_{n=1}^{\infty} \cos(\beta_n \eta) \left\{ \frac{S_n}{\beta_n^2} \left[\theta_{r,1} \left(e^{-\beta_n^2 (\tau_M - \tau_1)} - e^{-\beta_n^2 \tau_M} \right) + \sum_{m=1}^{M-1} \theta_{r,m+1} \left(e^{-\beta_n^2 (\tau_M - \tau_{m+1})} - e^{-\beta_n^2 (\tau_M - \tau_m)} \right) \right] - W_n \left[\theta_{r,1} e^{-\beta_n^2 \tau_M} + \sum_{m=1}^{M-1} (\theta_{r,m+1} - \theta_{r,m}) \, e^{-\beta_n^2 (\tau_M - \tau_m)} \right] \right\} + \frac{\eta^2 - 1}{2} \, Bi \theta_r \quad (11)$$

2.1.1 Model verification with numerical simulation

The analytical model is verified and validated with numerical simulation, the traditional CTF method and ANSI/ASHRAE Standard 140-2017. This section verifies the time-dependent temperature variations in a concrete slab as internal thermal mass using the finite-volume method [36]. The verification process is targeted to represent a case as general as possible. The thermal mass is assumed to be on the floor and has a thickness (L) of 0.3 m. The material density is 2500 kg m^{-3}. The thermal conductivity is 1.5 W m^{-1} K^{-1}. The specific heat is 750 J kg^{-1} K^{-1}. The nighttime ventilation rate is 1.5 h^{-1}. The hourly air temperatures are TMY3 dry bulb values between 19:00 and 07:00 hours in the night on November 13th in Long Island of California. The daily air temperature is the room setpoint temperature of 24°C that is also the initial temperature of the internal thermal mass.

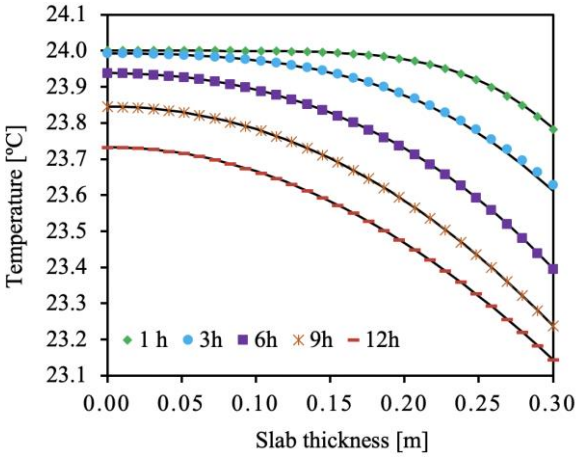

Fig 3. Temperature profiles at different hours: symbols and solid lines represents the results of the numerical simulation and the analytical model, respectively.

The finite-volume simulation was performed with the open source CFD code - OpenFOAM 7 and the laplacianFoam solver was used to solve the heat transfer in solids. The cell distance was chosen as $L/100$ uniformly based on both grid independence and sufficient resolution to compare with the analytical solution [26]. The time derivative was discretized with the first-order implicit scheme. The time step was chosen to satisfy the condition: $F_o\,(1+\xi Bi) \leqslant 0.5$, where $F_o = \lambda \Delta t/(\rho c \Delta^2 x)$, ξ is 0 and 1 for internal and boundary nodes, respectively, Δt is time step and Δx is cell distance. The time step is determined to be 3 seconds. The Laplacian term was discretized by the central-differencing scheme. The boundary and initial conditions have the form of (4-5).

Fig. 3 compares the temperature profiles obtained from the finite-volume method and the analytical model. The temperature profiles are shown along the thickness of the internal thermal mass at different hours. The theoretical model predicts the same temperature profiles as the numerical simulation. Both approaches show that the surface temperature (at 0.3 m) of the thermal mass is reduced by 0.2°C after 1 hour and 0.9°C after 12 hours. The bottom temperature of the slab starts to decrease after more than 3 hours and drops by 0.3°C after 12 hours.

2.1.2 ANSI/ASHRAE Standard 140 - Case 600 for model validation

ANSI/ASHRAE Standard 140 [30] is widely used in the building simulation community to validate models. Standard 140 documents the simulated energy demand of a thermal zone using different building energy simulation tools. In this study, Case 600 is presented for model validation. Case 600 is a lightweight cubic zone (6 m × 8 m × 2.7 m) with two windows (3 m × 2 m each) on the south wall. All details including materials and climate can be found in the section 5.2 in Standard 140-2017. Construction material properties are summarized in Appendix B. The U-value of the windows is 2.10 W m^{-2} K^{-1}. The internal heat gains are 200 W during all 24 hours per day for the full year. The internal heat gains are assumed 100% sensible and 60% radiative. The infiltration is 0.5 ACH. TMY3 weather data for Denver is used for the case. The setpoint temperature for cooling is 27°C. When nighttime cooling is applied to Case 600, the floor timer is changed to the concrete slab in section 2.1.1. Figure 4 compares the annual hourly integrated peak cooling loads predicted by the model in this study with those obtained from other two building simulation tools. The peak cooling load is 6.50 kW predicted in this study is in very close agreement with simulation results of other tools.

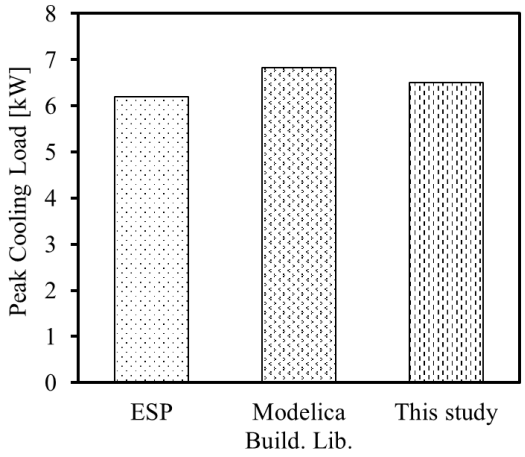

Fig 4. Case 600: peak cooling load at 13:00 on October 17th.

2.2. Nighttime cooling of internal thermal mass in different climates

The validated analytical model is used to study the capacity of nighttime cooling of internal thermal mass to reduce cooling demand in different climates. The sources of the hourly weather data are Typical Meteorological Year 3 (TMY3) and California Climate Zones 2 (CTZ2) data sets that also provide climate data for EnergyPlus. Forty-eight TMY3 and sixteen CTZ2 climate data are chosen to investigate the energy performance of nighttime mechanical ventilation of internal thermal mass in cities located in forty-eight U.S. states and across the sixteen climate zones in California, respectively. Filter criteria are applied to the climate data to ensure that it is beneficial to apply nighttime cooling: 1) the nightly average relative humidity is in the range of 20-70% [10];

2) average nightly temperatures are lower than 18 °C and the average monthly diurnal temperature range are higher than 7°C [10]; 3) Nighttime ventilation is activated from 21:00 hours in the night to 07:00 hours in the following day. The months for nighttime ventilation are picked based on these three criteria. The hourly temperature data between 7:00 and 21:00 in TMY3 and CTZ2 is replaced with the setpoint temperature 24°C. Figure 2 illustrates a sample temperature profile for the first 21 hours of a 24-h period. The first 3-day data is duplicated in the beginning of the weather file to eliminate the influence of the assumption of uniform temperature distribution in the thermal mass.

The heat removed from the internal thermal mass during the period of 10-h nighttime ventilation is used to indicate the capacity to shift and reduce cooling demand and defined as the total free cooling energy:

$$Q_s = \rho c_p H T_{init} \left\{ \sum_{n=1}^{\infty} \frac{sin\beta_n}{\beta_n} \Phi_{\mathrm{n}}(\tau_J) - \sum_{n=1}^{\infty} \frac{sin\beta_n}{\beta_n} \Phi_{\mathrm{n}}(\tau_K) + \frac{1}{3} Bi\left[\theta_r(\tau_K) - \theta_r(\tau_J)\right] \right\} \quad (12)$$

where, J and K express each start and end hour of nighttime ventilation for all months. Total free cooling energy is the sum of all positive values of free cooling energy storage (Q_s). The total free cooling days are the number of nights with positive values of free cooling energy and also used as a capacity indicator. When mechanical ventilation is used, there will be fan energy consumption. Therefore, two more capacity indicators are defined by considering fan energy consumption. The net free cooling energy is the sum of all positive values of the difference between free cooling energy storage and fan energy consumption. The net free cooling days are the number of nights in which free cooling energy is larger than fan energy consumption.

2.2.1 Estimation of mechanical fan energy consumption

An accurate calculation of fan energy consumption requires the detailed information of the mechanical system including pressure drop and airflow rates that vary from building to building and from system to system. Such detailed information is often hard to obtain, and simplified methods are needed to estimate fan energy consumption in a more general fashion. An alternative to characterize fan energy performance is to use the metric of fan efficacy that is defined as the power required to transport a fixed volume of air (W h m^{-3}) [10]. Springer et al. [10] summarized the fan efficacy of a central fan system. The total area of the internal thermal mass is assumed to be 200 m^2. The total volume flow rate is 4800 m^3 h^{-1} to maintain a high ventilation rate of 8 ACH that is average value for commercial buildings like schools according to CIBSE Guide B2 [37]. The total volume flow rate leads to a fan efficacy around 0.5 W h m^{-3}.

2.2.2 Validation of total free cooling energy

The total free cooling energy calculated by equation (12) is validated by the time-dependent heat fluxes at the slab surface calculated using CTF method [38]. The CTF method is based on Z-transform to compute solutions of transient heat transfer. It relates the current heat flux to past and present values of interior and exterior boundary temperatures (air or surface temperatures) as well as heat flux history. The heat flux (q'') at the slab" surface at the present time (t) is given by

$$q_t^{"} = X_0 T_{es,t} + \sum_{m=1}^{M_{es}} X_m T_{es,t-m\Delta t} - Y_0 T_{is,t} - \sum_{m=1}^{M_{is}} Y_m T_{is,t-m\Delta t} + \sum_{m=1}^{M_q} Z_m q_{t-m\Delta t}^{"} \quad (13)$$

where, X_m (W m^{-2} K^{-1}), Y_m (W m^{-2} K^{-1}), Z_m are conduction transfer function coefficients for exterior temperatures (T_{es}), interior temperatures (T_{is}), and past heat fluxes, respectively. In this study, the exterior temperatures are the above-mentioned hourly air temperatures. Δt is the time step. A difficult and complex task is to determine the conduction transfer coefficients. Seem [39] developed a detailed procedure for calculating CTF coefficients for one-dimensional slabs. The procedure is coded with Python to generate CTF coefficients and calculate heat flux at the slab surface. The Python code is verified by calculating CTF coefficients and heat fluxes at the exterior and interior surface of a single-layer material presented in the thesis of Seem. When CTF method is applied, it is necessary to assume past values of exterior temperatures, interior temperatures, and heat fluxes for the initial calculation. Then the calculation is iterated on the periodical air temperatures until a steady periodic solution is reached. In this study, the heat fluxes during the third 24 hours are used to verify the analytical model.

Table 1 Heat flux (W m^{-2}) at the surface of the slab

hour	CTFM	Analytical	Relative difference
19	4.780	4.725	0.01151
20	4.973	4.936	0.007440
21	5.123	5.092	0.006051
22	5.349	5.320	0.005422
23	5.713	5.684	0.005076
0	6.010	5.981	0.004825
1	6.375	6.345	0.004706
2	6.064	6.041	0.003793
3	5.830	5.810	0.003431
4	5.534	5.516	0.003253
5	5.376	5.360	0.002976
6	5.220	5.204	0.003065
7	-1.005	-0.9578	0.04697
8	-0.9321	-0.9100	0.02371
9	-0.8932	-0.8793	0.01556
10	-0.8666	-0.8572	0.01085
11	-0.8470	-0.8406	0.007556
12	-0.8320	-0.8278	0.005048
13	-0.8202	-0.8177	0.003048
14	-0.8107	-0.8094	0.001603
15	-0.8029	-0.8025	0.0004982
16	-0.7963	-0.7966	0.0003767
17	-0.7906	-0.7915	0.001138
18	-0.7855	-0.7868	0.001655

Table 1 compares the heat flux calculated with CTF methodand the analytical method. In general, a very good agreement is found between the two methods. The relative difference in the heat flux ranges from 0.00003767 to 0.04697. The maxima occurs when the exterior air temperature is switched from TMY3 dry bulb temperature (14.8°C) at 7:00 to the room setpoint temperature (24°C) at 8:00. In other words, the maximum difference in heat flux is due to the maximum exterior temperature difference between the previous and current hour. The CTF coefficients are obtained by spatially discretizing the slab into 51 resistances and 50 capacitances. The limited number of

resistance-capacitance finite-difference discretization would inevitably result in accuracy issues. The good agreement between the two methods indicate that the analytical model might be instrumental to optimize the CTF coefficients when the exterior temperatures have large gradients.

3. Results

3.1. Analytical model to assess nighttime cooling of internal thermal mass in Case 600

The analytical model is applied to evaluate the potential of nighttime cooling of the internal thermal mass in Case 600. Fig.5 shows the temperature profiles at different locations in the internal thermal mass for 216 hours from June 2nd to June 11th in Denver. The line y=0.30m represents the temperature variations of the floor surface, whereas the line y=0.05m represents a location near the adiabatic boundary. The grey line represents the time-dependent temperature variations of the room air. During the nighttime period (21:00-06:00), the room air temperature is calculated with equation (2). During the daytime period (07:00-20:00), the room air temperature is assumed to be the constant setpoint temperature (27°C). In the second full-day period in Fig.5, the room air temperature differs by 9.8°C during the nighttime, whereas the temperature variation of thermal mass surface is 2.4°C. The room air temperature cannot recover to the setpoint temperature 27°C at 08:00, but it is in the vicinity of 25°C that will not cause thermal discomfort. The lowest room air temperature is 13.7°C at 06:00 due to the lowest outdoor air temperature in the same hour. The thermal mass surface temperature reaches to its lowest value 19.8°C at 06:00 but the thermal mass temperature near the adiabatic surface reaches its lowest value 21.5°C in 4 hours later. The maximum temperature difference between the daytime and nighttime period is 3.7°C on the floor surface and 1.3°C at a depth of 0.15 m below the surface. The time-variation of the thermal mass temperature at depths of 0.15 m below the surface is only 33% of that on the surface. Therefore, a slab thickness of 0.15 m is optimum in terms of storing cooling energy during nighttime ventilation. The analytical model shows a great performance to calculate the dynamic temperature variations of the internal thermal mass under hourly varied and discrete air temperatures.

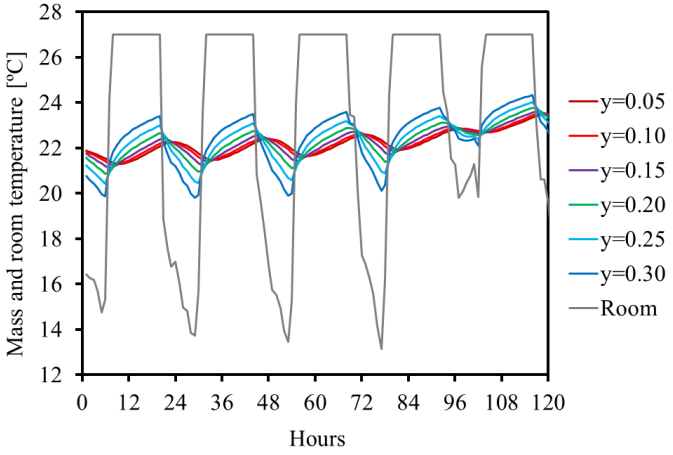

Fig. 5. Temperature variation at different locations of thermal mass in Case 600.

The daily cooling demand of Case 600 with and without nighttime cooling of internal thermal mass is shown in Fig.6. For the entire season requiring cooling, nighttime cooling of internal thermal mass can reduce daily cooling demand. The total cooling demand reduction is 1.2 MWh and about 26% of the annual cooling demand. The average daily cooling demand reduction is 7.3

kWh with a standard deviation of 2.4 kWh. The maximum reduction is 13.9 kWh and about 30% of the daily cooling demand. The maximum peak demand reduction is 1.4 kWh. For a specific day like June 3rd, the hourly peak demand (3.2 kWh) occurs at 15:00. Nighttime cooling of internal thermal mass can reduce peak cooling demand by 706.2 Wh that covers the peak cooling load of 640.5 W due to conduction heat gains through walls, roof and windows, internal and infiltration heat gains.

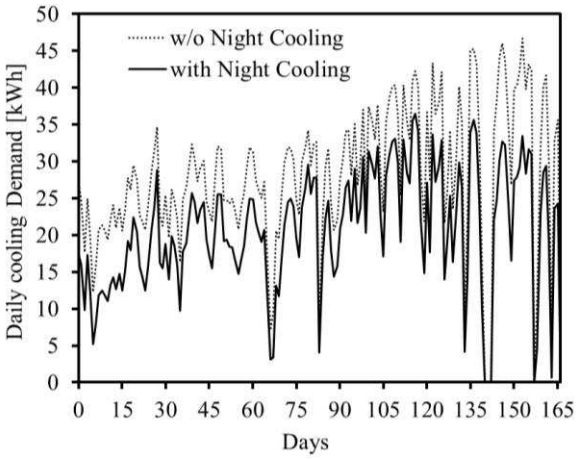

Fig. 6. Total cooling demand for Case 600 with and without nighttime cooling of internal thermal mass.

3.2. Capacity of nighttime cooling of internal thermal mass in different U.S. climates

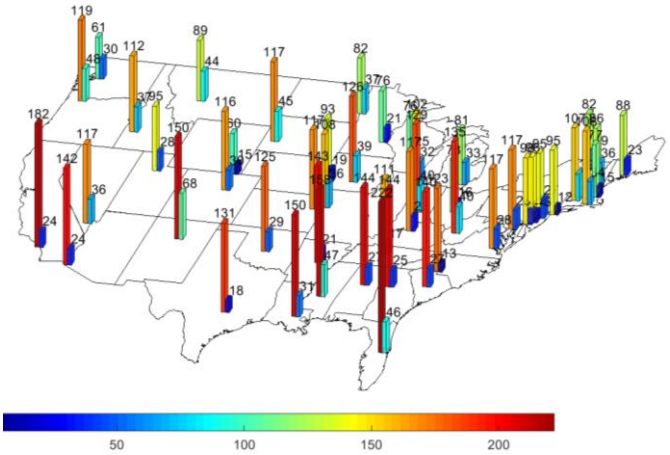

Fig 7. Total and net free cooling days in different U.S. cities.

The analytical model is applied to evaluate the potential of nighttime mechanical ventilation of building internal thermal mass by calculating total and net free cooling days in different U.S. cities (Fig 7). In general, the number of total free cooling days decreases from southern states to northern states. This is associated to the change in the climate zones with latitude. In the southern U.S. region with hot-dry or hot humid climate, the average value of annual total and net free-cooling-days is 160 and 28, respectively. In the middle U.S. region with mixed humid climate, the average value of annual total and net free-cooling-days is 121 and 24, respectively. In the northern U.S. regions with cold climate, the average value of annual total and net free-cooling-days is 98 and 32, respectively.

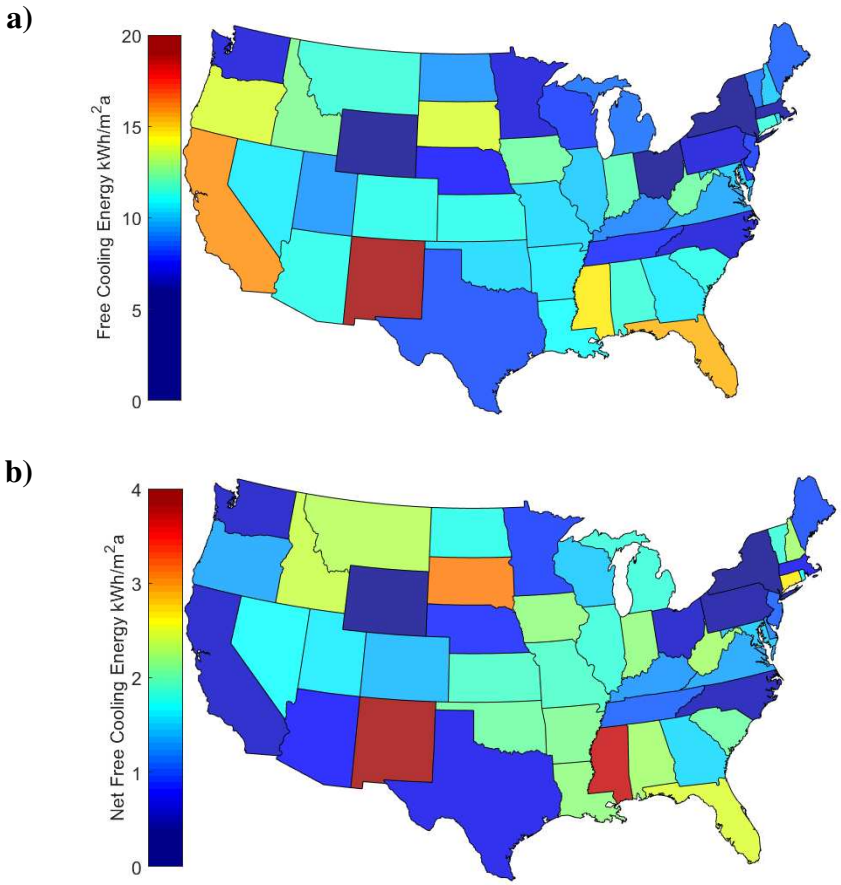

Fig. 8. a) Total and b) net free cooling energy storage in different U.S. cities.

For a region with hot-dry climate, the range of annual total free-cooling-days is from 117 to 182, while the range of annual net free-cooling-days is from 24 to 36. For example, the total free cooling days are 117 in Las Vegas, AZ, but the net energy saving is achieved for only 36 days. This is due to high average nighttime temperature of 20°C during the ventilation period. The total and net free cooling days are 117 and 24, respectively, in Long Beach, CA. For a region with hot-humid climate, the range of annual total free-cooling-days is from 131 to 222, while the range of annual net free-cooling-days is from 3 to 47. For example, the total free cooling days are 222 in Orlando, FL, while net energy saving is achieved in 47 of those days. The total and net free cooling days are 179 and 3, respectively, in Honolulu, HI. The small number of net free cooling days in Honolulu is due to the high average nighttime temperature of 23°C during the ventilation period. For a region with marine climate, two cities are selected to demonstrate the potential of nighttime mechanical ventilation of internal thermal mass. In Seattle, WA, the total free cooling days are only 61, and net cooling storage is achieved in 50% of those nights. In Portland, OR, the total free cooling days increase to 119, but the net cooling storage is achieved in only 48 nights. For a region with mixed humid climate, total free cooling days range from 95 to 135, while most of the net free cooling days are below 30. Among the 15 tested cities in the mixed-humid climate zone, only Charleston, WV and Kansas City, MO have net cooling days of more than 30 days. In eastern coastal cities such as New York, the net free cooling days are only 12. For a region with cold or very cold climate, the total free cooling days range from 60 to 150, while the net free cooling days range from 15 to 68. Cheyenne, WY has least net free cooling days of 15 due to too cold nighttime

temperature. Santa Fe, NM has 68 net free cooling days and shows most promising to flush internal thermal mass with nighttime mechanical ventilation.

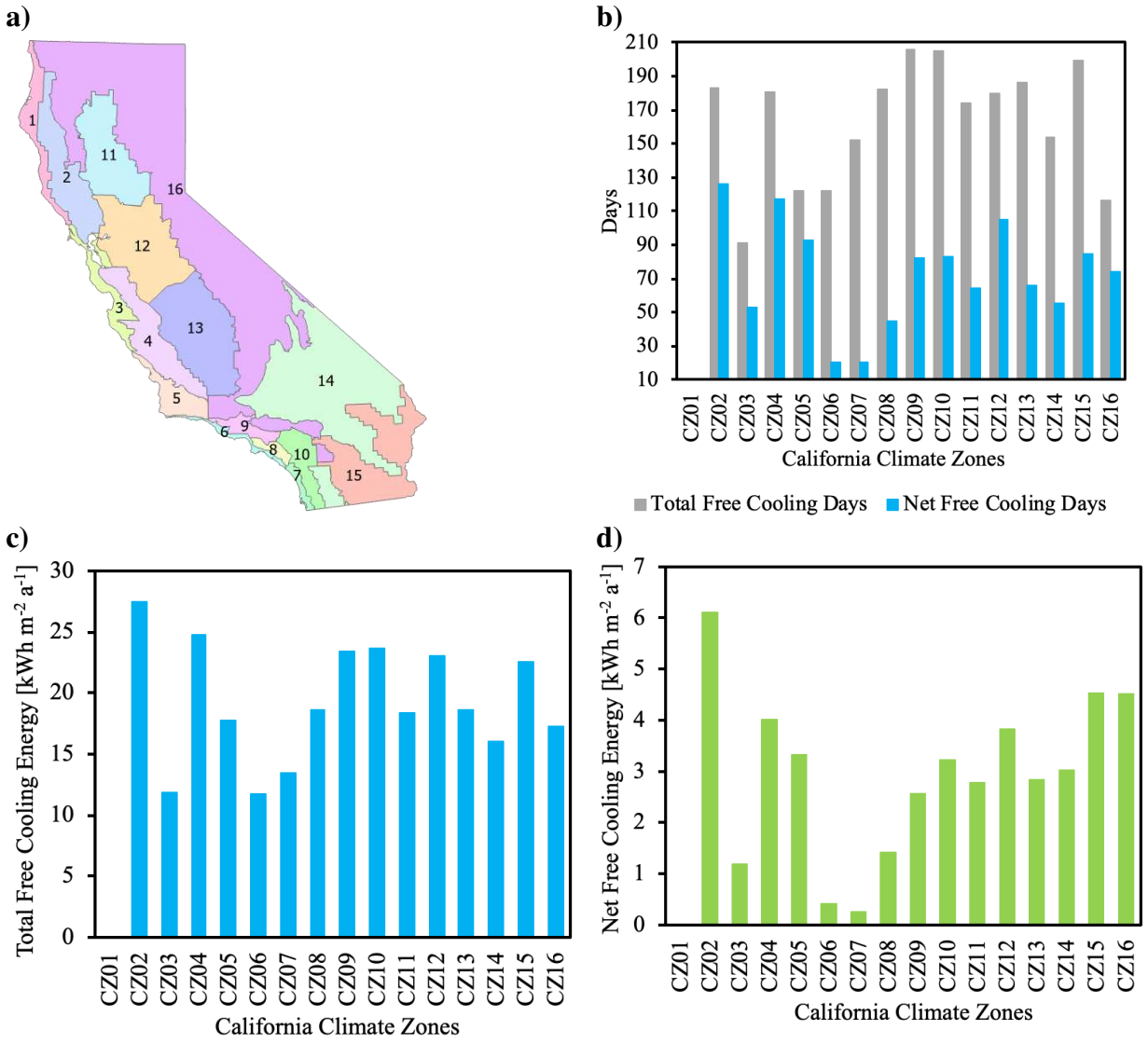

Fig. 9. a) California climate zone. b) total and net free cooling days, c) total and d) net free cooling energy storage in different California climate zones.

The analytical model is further applied to quantify the total and net free cooling energy storage in 48 different U.S. cities (Fig. 8). The value of the total and free cooling energy storage in each city is used to contour the corresponding state. Compared to total free cooling days, the total free cooling energy storage does not show a decreasing trend from southern states to northern states. For all the three cities (Yuma, Long Beach and Las Vegas) with hot-dry climate, the total free cooling energy storage is above 10 kWh m^{-2} per year, while the fan energy consumption is more than 80% of the total free cooling energy. For a region with hot-humid climate, the stored total free cooling energy ranges from 6.82 to 15.3 kWh m^{-2} per year, while the net free cooling energy accounts for less than 26%. In Honolulu, HI, the net free cooling energy is nearly 0 kWh m^{-2} per year. High total free cooling energy does not necessarily lead to high net free cooling energy. For example, the total free cooling energy in Orlando, FL, is 15.3 kWh m^{-2} per year that is higher than

14.7 kWh m^{-2} per year in Jackson, MS. On the contrary, the net free cooling energy in Orlando is 2.48 kWh m^{-2} per year and lower than 3.74 kWh m^{-2} per year in Jackson. In Portland and Seattle with marine climate, the average total cooling energy is 10.4 kWh m^{-2} per year, while the fan energy consumption accounts for more than 90%. For a region with mixed humid climate, the minimum total (5.86 kWh m^{-2} a^{-1}) and net (0.39 kWh m^{-2} a^{-1}) free cooling energy storage is reported in New York. Birmingham, AL, has the maximum net free cooling energy storage of 2.24 kWh m^{-2} per year, while the maximum total free cooling energy storage of 12.3 kWh m^{-2} per year is found Charleston, WV. For a region with cold or very cold climate, the total free cooling energy ranges from 6.08 to 19.1 kWh m^{-2} per year, while the net free cooling energy ranges from 0.34 to 3.88 kWh m^{-2} per year. The maximum total and net free cooling energy are reported in Santa Fe, NM. Comparing to Santa Fe, Rapid City, SD, has a lower total free cooling energy of 13.7 kWh m^{-2} per year, but the net free cooling energy of 3.11 kWh m^{-2} per year is more similar.

Finally, the analytical model is applied to elaborate the free cooling energy storage in different California climate zones (Fig. 9). In general, it is not suitable to apply nighttime ventilation of internal thermal mass in coastal regions including climate zone CZ01, CZ03, CZ06 and CZ07. The total free cooling days is determined as zero in CZ01. Despite an average total free cooling energy of 12.4 kWh m^{-2} per year in CZ03, CZ06 and CZ07, the average net free cooling energy of 0.62 kWh m^{-2} per year indicates fan energy consumption accounts for 95%. In regions further into the land, nighttime ventilation of internal thermal mass shows better performance. The total free cooling days range from 116 to 206, while the net free cooling days range from 55 to 126. The total free cooling energy storage is above 17.2 kWh m^{-2} per year for these climate zones. Especially in CZ02, the total free cooling energy storage achieves 27.5 kWh m^{-2} per year, while the net free cooling energy is 6.11 kWh m^{-2} per year.

4. Discussion

The research on nighttime cooling of internal thermal mass is limited due to lacking simplified models by considering mass dimension and real-world discrete climate data like hourly outdoor air temperatures. The analytical model in this study is developed to evaluate the performance of nighttime cooling of internal thermal mass with discrete (hourly varied) air temperature boundary conditions. It has a potential to be integrated into whole building energy simulation software, such as EnergyPlus that sets internal thermal mass either as an effective area or a capacitance multiplier for the zonal air. EnergyPlus predicts hourly zonal air temperature that can be coupled with the analytical model. The temperature of the zonal air and the internal thermal mass can be updated by iteration method. The fan energy consumption in this study is roughly estimated with fan efficacy curve that affects the accuracy on quantifying net free cooling energy storage. Once the analytical model is integrated into EnergyPlus, the fan energy can be simulated in details and the estimation accuracy of the net free cooling energy can also be improved. The analytical model has some advantages over existing simplified models and the methods dealing with internal thermal mass in whole building energy simulation software. For example, the simplified model [28] predicts the same temperature variation of room air and thermal mass due to the ignorance of thermal mass dimension. The analytical model shows that the lag in temperature variation between thermal mass and room air can be up to 4 hours (Fig.5). The ignorance of internal thermal mass dimension like EnergyPlus multiplier method may lead to exaggerate the efficiency of internal thermal mass for energy storage and such overestimation can be overcome by the integration of the proposed analytical model in this study. The standalone analytical model can also be used to

quantify the free cooling energy storage with hourly temperature data without knowing the details of building components, construction materials and etc. The limitation of the analytical model is the requirement of constant ACH. The present form can be used only for constant-air-volume system. Through the analysis of the total free cooling energy storage under different U.S. climates, it will be very useful to further explore the performance of nighttime ventilation of internal thermal mass with both hourly varied ventilation rates and air temperatures.

The analytical model is then applied to evaluate the performance of nighttime mechanical ventilation of building internal thermal mass in different U.S. climate zones by total free cooling days, net free cooling days, total free cooling energy storage and net free cooling energy. Total free cooling days might be a good index to indicate energy flexibility. Total free cooling days are above 60 days per year for all the 48 tested cities. It means that nighttime mechanical ventilation of internal thermal mass can be designed to shift peak cooling demand for at least two months. The dependency of total free cooling days on climate zones is not obvious (Fig. 7). It indicates that analyzing only climate data is not adequate to evaluate the energy flexibility of nighttime cooling. Therefore, total free cooling energy can be further used to quantify the energy flexibility. The total free cooling energy is above 10 kWh m^{-2} per year for 27 cities. Liu et al. [40] reported that the energy demand of zero energy buildings should be less than 15 kWh m^{-2} per year. Therefore, design of nighttime mechanical ventilation and internal thermal mass is able to provide more than 67% useful energy demand for those type of buildings in the 27 cities. Nighttime cooling of internal thermal mass is indeed promising in terms of energy flexibility for many U.S. climate zones. Net free cooling days might be a good index to indicate energy savings. The difference in net free cooling days is small between cities in various U.S. climate zones. Net free cooling days range from 10 to 40 days for most cities. Santa Fe has the largest number of net free cooling days of 68 days per year and Honolulu has the smallest number of net free cooling days of only 3 days per year. Hence, applying nighttime mechanical ventilation of internal thermal mass is not an ideal solution for energy saving purpose. Energy saving can be further quantified by net free cooling energy. The maximum net free cooling energy in the 48 cities is 3.88 kWh m^{-2} per year. If the maximum energy demand of zero energy buildings is still used as reference, a maximum energy saving of 26% can be achieved. A comparison between the total and net free cooling energy under different U.S. climates enlightens that nighttime natural ventilation of internal thermal mass might be a more suitable alternative for energy saving. Different locations in the same state might be in different climate zones, for example, California has 16 climate divisions. Free cooling days and energy storage in a single city of a state is not adequate to reveal the general pattern of the nighttime mechanical ventilation of internal thermal mass under different U.S. climates. Therefore, the free cooling days and energy storage are quantified for all the 16 climate zones in California. The more detailed calculation offers new insights on nighttime mechanical ventilation of internal thermal mass and the performance becomes better from coast regions further into the land. The maximum total and net free cooling energy in California are about 1.5 times of those in Santa Fe.

The development of the analytical model is to implement the evaluation of capacity of the nighttime cooling of the internal thermal mass to reduce cooling demand in different U.S. climates. One main purpose to manage energy demand is to create energy flexibility for increasing the integration of renewable energy. The energy flexibility created by nighttime cooling of internal thermal mass is demonstrated using ANSI/ASHRAE Standard 140 – Case 600 in Denver climate. The shifting efficiency ($\eta_{shifting}$) proposed by Dréau and Heiselberg [31] is adopted here to assess

464 the energy flexibility. Fig.10 shows the shifting efficiency of the nighttime cooling of internal
465 thermal mass for Case 600. The efficiency lower than one means that not all stored cooling energy
466 are used in the same day but shifted to the following day. The average efficiency during the cooling
467 demand season is 0.9 with a standard deviation of 0.3. The range of the efficiency is 0.4 ~ 2.2 and
468 a similar range is also reported by Dréau and Heiselberg [31]. It is observed that the maximum
469 efficiency is 2.2 followed by 12 days with an average efficiency 0.7, which shows the capacity of
470 the nighttime cooling of the internal thermal mass to create energy flexibility.

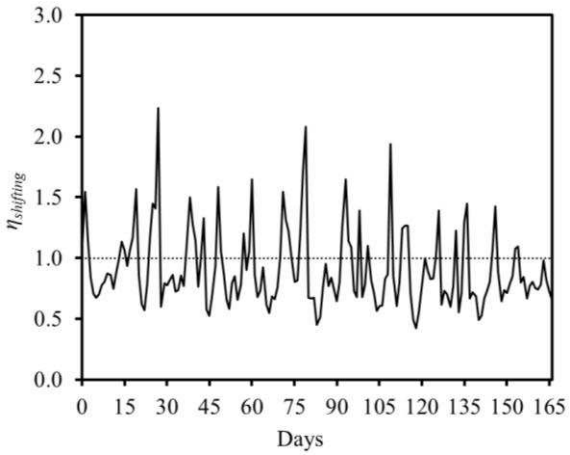

471

472 **Fig. 10. Shifting efficiency of nighttime cooling of internal thermal mass to create energy flexibility.**

473 ## 5. Conclusions

474 The research on nighttime cooling of internal thermal mass is limited due to lacking simplified
475 models by considering mass dimension and real-world discrete climate data like outdoor air
476 temperatures. This study develops a one-dimensional analytical model for nighttime mechanical
477 ventilation of internal thermal mass in buildings with a fixed air change rate, and constant air
478 temperature in the daytime period but hourly varied air temperatures in the nighttime period.
479 Temperature profiles for a general case obtained from the analytical model is confirmed by the
480 results from time-dependent numerical simulations with the same boundary and initial conditions.
481 The validated model is used to explore the free cooling energy storage of internal thermal mass
482 during nighttime flush, and the main observations are:

483 1) Nighttime mechanical ventilation of internal thermal mass can be designed to shift peak
484 cooling demand for at least two months for most locations. This is indicated by the total free
485 cooling days, which are above 60 days per year for all the 48 cities tested. Among these U.S.
486 cities in different climate zones, the maximum free cooling energy storage (19.1 kWh m^{-2} a^{-1})
487 is reported in Santa Fe, NM. Furthermore, the total free cooling energy is above 10 kWh m^{-2}
488 per year for 27 selected cities, suggesting that they are suitable to apply nighttime cooling of
489 internal thermal mass to shift peak cooling demand.
490 2) The energy savings by adopting nighttime mechanical ventilation of internal thermal mass is
491 not exceptional when fan energy consumption is taken into account. Net free cooling days
492 range from 10 to 40 days for different cities. Honolulu has the smallest number of net free
493 cooling days with only 3 days per year. Santa Fe has the largest number of net free cooling
494 days of 68 days per year. Santa Fe also has the maximum net free cooling energy of 3.88 kWh

m^{-2} a^{-1}. It is essential to reduce fan energy consumption to improve energy saving potential of internal thermal mass.

3) Free cooling energy quantified for the 16 climate zones in California shows that coastal regions are not suitable for nighttime mechanical ventilation of internal thermal mass. Large variation among different regions demonstrate that ventilation strategies need to be customized for different climate zones. The maximum total free cooling energy storage in California achieves 27.5 kWh m^{-2} a^{-1}, while the maximum net free cooling energy is 6.11 kWh m^{-2} a^{-1}.

The analytical model developed is convenient to examine the efficacy of nighttime mechanical ventilation of internal thermal mass to create energy flexibility. In addition to quantification of free cooling energy storage shown in this study, this model has the potential to be integrated into whole building energy simulation software to improve the efficiency and accuracy of evaluating the impact of internal thermal mass on indoor air temperature.

Acknowledgement

Dr. Wu would like to acknowledge the support of the National Science Foundation through Award Number: 2100781.

Appendix A. Derivation of the analytical model

Equation (4) can be normalized as:

$$\frac{\partial \theta}{\partial \tau} = \frac{\partial^2 \theta}{\partial \eta^2} \tag{A1}$$

$$-\frac{\partial \theta}{\partial \eta}\Big|_{\eta=1} = Bi[\theta(\eta = 1, \tau) - \theta_r(\tau)] \tag{A2}$$

$$\frac{\partial \theta}{\partial \eta}\Big|_{\eta=0} = 0 \tag{A3}$$

$$\theta(\eta, 0) = \theta_r(0) = 0 \tag{A4}$$

Shifting function method is applied to find the solution to equation (A1) with an inhomogeneous Robin boundary condition (A2). The solution takes the following form:

$$\theta = \Psi(\eta, \tau) + u(\tau)v(\eta) \tag{A5}$$

where $v(\eta)$ is a shifting function and $u(\tau)$ contains time-dependent boundary values. The following equations are obtained by substituting equation (A5) into equation (A1-3):

$$\frac{\partial \Psi}{\partial \tau} + \frac{du}{d\tau} = \frac{\partial^2 \Psi}{\partial \eta^2} + u\frac{d^2 \mathrm{v}}{d\eta^2}$$

$$\eta = 1: \quad -\frac{\partial \Psi}{\partial \eta} - u\frac{dv}{d\eta} = Bi(\Psi + uv - \theta_r) \tag{A6}$$

$$\eta = 0: \quad \frac{\partial \Psi}{\partial \eta} + u\frac{dv}{d\eta} = 0$$

To make the Robin boundary condition homogeneous, u and v take the following form:

$$u = Bi\theta_r \tag{A7}$$

$$v = \frac{\eta^2 - 1}{2} \tag{A8}$$

517 The one-dimensional heat equation is recast as

$$\frac{\partial \Psi}{\partial \tau} = \frac{\partial^2 \Psi}{\partial \eta^2} + Bi\theta_r - \frac{1}{2}Bi(\eta^2 - 1)\frac{d\theta_r}{d\tau} \tag{A9}$$

518 Equation (A9) can be solved by using Separation of Variables and Fourier series expansion. The
519 separated function for space dimension satisfies homogeneous boundary conditions. The solution
520 takes the following form:

$$\Psi = \sum_{n=1}^{\infty} \cos(\beta_n \eta)\, \Phi_{\mathrm{n}}(\tau) \tag{A10}$$

521 where the eigenvalues β_n are the roots of the transcendental equation

$$\beta_n \sin(\beta_n) = Bi\cos(\beta_n) \tag{A11}$$

522 Since the initial values of equation (A9) are zero, Φ can be determined by using the variation of
523 parameters (VOP) method [26] and the principle of orthogonality:

$$\Phi_{\mathrm{n}} = \frac{1}{R_n}\int_0^1 \Psi\cos(\beta_n \eta)\mathrm{d}\eta$$
$$R_n = \int_0^1 cos^2(\beta_n \eta)\mathrm{d}\eta = \frac{\beta_n^2 + Bi^2 + Bi}{2(\beta_n^2 + Bi^2)} \tag{A12}$$

524 The essence of VOP is to differentiate equation (A12) with respect to time and replace the partial
525 derivative with the right-hand side of equation (A9). An ordinary differential equation (ODE) for
526 Φ is obtained after carrying out the integration:

$$\frac{d\Phi_{\mathrm{n}}}{d\tau} = -\beta_n^2 \Phi_{\mathrm{n}} + S_n\theta_r - W_n\frac{d\theta_r}{d\tau} \tag{A13}$$

$$S_n = \frac{Bi\sin(\beta_n)}{R_n\beta_n}$$
$$W_n = \frac{Bi(\cos\beta_n - sin\beta_n/\beta_n)}{R_n\beta_n^2} \tag{A15}$$

527 Employing the integral properties of Dirac delta function, the ODE can be expressed in the
528 following summation form:

$$\Phi_{\mathrm{n}} = \frac{S_n}{\beta_n^2}\left\{\theta_{r,1}\left(e^{-\beta_n^2(\tau_M - \tau_1)} - e^{-\beta_n^2\tau_M}\right) + \sum_{m=1}^{M-1}\theta_{r,m+1}\left(e^{-\beta_n^2(\tau_M - \tau_{m+1})} - e^{-\beta_n^2(\tau_M - \tau_m)}\right)\right\} \tag{A16}$$
$$- W_n\left\{\theta_{r,1}e^{-\beta_n^2\tau_M} + \sum_{m=1}^{M-1}(\theta_{r,m+1} - \theta_{r,m})\, e^{-\beta_n^2(\tau_M - \tau_m)}\right\}$$

Substituting Equation (A7-8) (A10) (A16) into Equation (A5), the final analytical model for nighttime cooling of internal thermal mass is obtained as equation (11).

Appendix B. Simulation details of Case 600

Table B1 Thermal properties of construction materials

Material (Inside to Outside)	λ W m^{-1} K^{-1}	ρ kg m^{-3}	specific heat J kg^{-1} K^{-1}	Thickness m
Exterior Wall				
Plasterboard	0.16	950	840	0.012
Fiberglass quilt	0.04	12	840	0.066
Wood siding	0.14	530	900	0.009
Floor				
Timber	0.14	650	1200	0.025
Insulation	0.04	-	-	1.003
Roof				
Plasterboard	0.16	950	840	0.010
Fiberglass quilt	0.04	12	840	0.1118
Roof deck	0.14	530	900	0.019

References

[1] M. Saffari, C. Roe, D.P. Finn, Improving the building energy flexibility using PCM-enhanced envelopes, Appl. Therm. Eng. 217 (2022) 119092. https://doi.org/https://doi.org/10.1016/j.applthermaleng.2022.119092.

[2] P.H. Feng, B.C. Zhao, R.Z. Wang, Thermophysical heat storage for cooling, heating, and power generation: A review, Appl. Therm. Eng. 166 (2020) 114728. https://doi.org/https://doi.org/10.1016/j.applthermaleng.2019.114728.

[3] E. Alptekin, M.A. Ezan, Performance investigations on a sensible heat thermal energy storage tank with a solar collector under variable climatic conditions, Appl. Therm. Eng. 164 (2020) 114423. https://doi.org/https://doi.org/10.1016/j.applthermaleng.2019.114423.

[4] S. Verbeke, A. Audenaert, Thermal inertia in buildings: A review of impacts across climate and building use, Renew. Sustain. Energy Rev. 82 (2018) 2300–2318. https://doi.org/10.1016/j.rser.2017.08.083.

[5] A. Reilly, O. Kinnane, The impact of thermal mass on building energy consumption, Appl. Energy. 198 (2017) 108–121. https://doi.org/10.1016/j.apenergy.2017.04.024.

[6] F. Stazi, E. Tomassoni, C. Bonfigli, C. Di Perna, Energy, comfort and environmental assessment of different building envelope techniques in a Mediterranean climate with a hot dry summer, Appl. Energy. 134 (2014) 176–196. https://doi.org/10.1016/j.apenergy.2014.08.023.

[7] L. Zhu, R. Hurt, D. Correia, R. Boehm, Detailed energy saving performance analyses on thermal mass walls demonstrated in a zero energy house, Energy Build. 41 (2009) 303–310. https://doi.org/https://doi.org/10.1016/j.enbuild.2008.10.003.

[8] J. Landsman, G. Brager, M. Doctor-Pingel, Performance, prediction, optimization, and user behavior of night ventilation, Energy Build. 166 (2018) 60–72.

https://doi.org/https://doi.org/10.1016/j.enbuild.2018.01.026.

[9] A. Gagliano, F. Patania, F. Nocera, C. Signorello, Assessment of the dynamic thermal performance of massive buildings, Energy Build. 72 (2014) 361–370. https://doi.org/https://doi.org/10.1016/j.enbuild.2013.12.060.

[10] D. Springer, B. Dakin, A. German, Measure Guideline: Ventilation Cooling, Davis, California, 2012.

[11] E. Solgi, Z. Hamedani, R. Fernando, H. Skates, N.E. Orji, A literature review of night ventilation strategies in buildings, Energy Build. 173 (2018) 337–352. https://doi.org/https://doi.org/10.1016/j.enbuild.2018.05.052.

[12] H. Johra, P. Heiselberg, J. Le Dréau, Influence of envelope, structural thermal mass and indoor content on the building heating energy flexibility, Energy Build. 183 (2019) 325–339. https://doi.org/10.1016/j.enbuild.2018.11.012.

[13] Y. Liu, L. Yang, L. Hou, S. Li, J. Yang, Q. Wang, A porous building approach for modelling flow and heat transfer around and inside an isolated building on night ventilation and thermal mass, Energy. 141 (2017) 1914–1927. https://doi.org/10.1016/j.energy.2017.11.137.

[14] H. Campaniço, P. Hollmuller, P.M.M. Soares, Assessing energy savings in cooling demand of buildings using passive cooling systems based on ventilation, Appl. Energy. 134 (2014) 426–438. https://doi.org/10.1016/j.apenergy.2014.08.053.

[15] T. Kuczyński, A. Staszczuk, Experimental study of the influence of thermal mass on thermal comfort and cooling energy demand in residential buildings, Energy. 195 (2020). https://doi.org/10.1016/j.energy.2020.116984.

[16] R. Lindberg, A. Binamu, M. Teikari, Five-year data of measured weather, energy consumption, and time-dependent temperature variations within different exterior wall structures, Energy Build. 36 (2004) 495–501. https://doi.org/https://doi.org/10.1016/j.enbuild.2003.12.009.

[17] E. Rodrigues, M.S. Fernandes, A.R. Gaspar, Á. Gomes, J.J. Costa, Thermal transmittance effect on energy consumption of Mediterranean buildings with different thermal mass, Appl. Energy. 252 (2019) 113437. https://doi.org/10.1016/j.apenergy.2019.113437.

[18] W.J.N. Turner, I.S. Walker, J. Roux, Peak load reductions: Electric load shifting with mechanical pre-cooling of residential buildings with low thermal mass, Energy. 82 (2015) 1057–1067. https://doi.org/10.1016/j.energy.2015.02.011.

[19] T. Kalema, G. Jhannesson, P. Pylsy, P. Hagengran, Accuracy of energy analysis of buildings: A comparison of a monthly energy balance method and simulation methods in calculating the energy consumption and the effect of thermal mass, J. Build. Phys. 32 (2008) 101–130. https://doi.org/10.1177/1744259108093920.

[20] F. Leccese, G. Salvadori, F. Asdrubali, P. Gori, Passive thermal behaviour of buildings: Performance of external multi-layered walls and influence of internal walls, Appl. Energy. 225 (2018) 1078–1089. https://doi.org/10.1016/j.apenergy.2018.05.090.

[21] B. Bozkaya, R. Li, T. Labeodan, R. Kramer, W. Zeiler, Development and evaluation of a building integrated aquifer thermal storage model, Appl. Therm. Eng. 126 (2017) 620–629. https://doi.org/https://doi.org/10.1016/j.applthermaleng.2017.07.195.

[22] S.A. Al-Sanea, M.F. Zedan, S.N. Al-Hussain, Effect of thermal mass on performance of insulated building walls and the concept of energy savings potential, Appl. Energy. 89 (2012) 430–442. https://doi.org/10.1016/j.apenergy.2011.08.009.

[23] W. Wu, T. Defraeye, Identifying heterogeneities in cooling and quality evolution for a pallet of packed fresh fruit by using virtual cold chains, Appl. Therm. Eng. 133 (2018). https://doi.org/10.1016/j.applthermaleng.2017.11.049.

[24] K. Shan, J. Wang, M. Hu, D. ce Gao, A model-based control strategy to recover cooling energy from thermal mass in commercial buildings, Energy. 172 (2019) 958–967. https://doi.org/10.1016/j.energy.2019.02.045.

[25] M.J.N. Oliveira Panão, N.M. Mateus, G. Carrilho da Graça, Measured and modeled performance of internal mass as a thermal energy battery for energy flexible residential buildings, Appl. Energy. 239 (2019) 252–267. https://doi.org/10.1016/j.apenergy.2019.01.200.

[26] W. Wu, W. Zhang, J. Benner, A. Malkawi, Critical evaluation of analytical methods for thermally activated building systems, Renew. Sustain. Energy Rev. 117 (2020) 109516. https://doi.org/https://doi.org/10.1016/j.rser.2019.109516.

[27] A. Jeanjean, R. Olives, X. Py, Selection criteria of thermal mass materials for low-energy building construction applied to conventional and alternative materials, Energy Build. 63 (2013) 36–48. https://doi.org/https://doi.org/10.1016/j.enbuild.2013.03.047.

[28] L. Yang, Y. Li, Cooling load reduction by using thermal mass and night ventilation, Energy Build. 40 (2008) 2052–2058. https://doi.org/10.1016/j.enbuild.2008.05.014.

[29] B. Delcroix, M. Kummert, A.. Daoud, M. Hiller, Improved Conduction Transfer Function Coefficients Generation in TRNSYS Multizone Building Model, in: Prroceedings of BS2013, Cambery, France, 2013: pp. 2667–2674.

[30] N.J. Kruis, M. Kummert, R.T. Muehleisen, J.F. Pegues, J. Neymark, T.P. Mcdowell, M.J. Witte, A. Roth, P. Strachan, M. Tosh, C.S. Barnaby, R.B. Burkhead, S.S. Hanson, Standard method of test for the evaluation of building energy analysis computer programs, ASHRAE Stand. 8400 (2004).

[31] J. Le Dréau, P. Heiselberg, Energy flexibility of residential buildings using short term heat storage in the thermal mass, Energy. 111 (2016) 991–1002. https://doi.org/10.1016/j.energy.2016.05.076.

[32] D.F. Dominković, P. Gianniou, M. Münster, A. Heller, C. Rode, Utilizing thermal building mass for storage in district heating systems: Combined building level simulations and system level optimization, Energy. 153 (2018) 949–966. https://doi.org/10.1016/j.energy.2018.04.093.

[33] M. Hu, F. Xiao, J.B. Jørgensen, R. Li, Price-responsive model predictive control of floor heating systems for demand response using building thermal mass, Appl. Therm. Eng. 153

(2019) 316–329. https://doi.org/https://doi.org/10.1016/j.applthermaleng.2019.02.107.

[34] W. Wu, Z. Tong, G. Zhang, A. Malkawi, X. Wang, J. Benner, An energy efficient hydraulic system to cool manure and reduce ammonia emissions from livestock buildings, J. Clean. Prod. 235 (2019) 920–929. https://doi.org/https://doi.org/10.1016/j.jclepro.2019.07.036.

[35] T.W. Tu, S.Y. Lee, A New Analytic Solution for the Heat Conduction with Time-Dependent Heat Transfer Coefficient, Int. J. Mech. Mechatronics Eng. 8 (2014) 1392–1397.

[36] W. Wu, Z. Tong, G. Zhang, A. Malkawi, X. Wang, J. Benner, An energy efficient hydraulic system to cool manure and reduce ammonia emissions from livestock buildings, J. Clean. Prod. 235 (2019). https://doi.org/10.1016/j.jclepro.2019.07.036.

[37] CIBSE, CIBSE Guide B2 Ventilation and ductwork, CIBSE, 2016.

[38] F.C. McQuiston, J.D. Parker, Heating, Ventiling and Air Conditioning, Analysis and Design, Sixth, John Wiley and Sons, New York, 1994.

[39] J.E. Seem, Modeling of Heat Transfer in Buildings, University of Wisconsin-Madison, 1987.

[40] Z. Liu, Y. Liu, B.J. He, W. Xu, G. Jin, X. Zhang, Application and suitability analysis of the key technologies in nearly zero energy buildings in China, Renew. Sustain. Energy Rev. 101 (2019) 329–345. https://doi.org/10.1016/j.rser.2018.11.023.